Digest Journal of Nanomaterials and Biostructures Vol. 16, No. 3, July - September 2021, p. 915 - 928

Study on plasma-spraying of MCrAlY coatings

Z. L. Wang[a], Q. Li[b], C. Ju[a], Q. H. Song [a], Z. P. Sun[a], Y. F. Zhang[a,*]
[a]*School of Mechanical & Automotive Engineering, Qilu University of Technology, Shandong Academy of Sciences, Jinan, Shandong, 250353, PR China*
[b]*School of Material Science & Engineering, Qilu University of Technology, Shandong Academy of Sciences, Jinan, Shandong, 250353, PR China*

In this paper, two kinds of MCrAlY coatings were prepared by atmospheric plasma spraying. The powders and coatings were characterized with scanning electron microscopy and energy dispersive spectrometry. X-ray diffraction and thermogravimetry differential thermal analysis were used to qualitatively analyze the phase. The change of powder mass with time and the change of heat absorption and exothermic were measured, and then the generation of new material was analyzed. It was found that the melting effect of the two kinds of powder by plasma spraying was good, and coating with high temperature oxidation resistance and hot corrosion resistance can be prepared. Both powders weight increased when heated in air, which indicates that oxidation occurs when the temperature rose. The main composition of NiCrAlY coating was γ'-Ni_3Al, while NiCoCrAlYTa coating contained several kinds of NiAl composites.

(Received March 2, 2021; Accepted August 3, 2021)

Keywords: APS, MCrAlY coating, NiCrAlY, NiCoCrAlYTa

1. Introduction

MCrAlY alloy is a kind of alloy which is formed by Co, Ni, Fe or their combination as basic elements, Al, Cr as oxide film elements, adding Y, Hf, Ta, Si and other trace active elements [1]. MCrAlY alloy is mainly used as bond coat (BC) of thermal barrier coatings (TBCs) for aerospace engines and gas turbines to prevent substrate oxidation [2]. It has good oxidation resistance and strong adhesion [3-5]. At high temperature, the oxidation of BC can also make the interface between ceramic layer and adhesive layer form Thermally Grown Oxide (TGO). The TGO layer is mainly composed of Al_2O_3, which can further improve the service life of TBCs [6]. BC can be prepared on the surface of superalloy substrate by atmospheric plasma spraying (APS), low pressure plasma spraying (LPPS) or electron beam physical vapor deposition (EB-PVD) [7]. In addition, MCrAlY has good toughness, high strength, high temperature oxidation resistance and hot corrosion resistance, and can also be used as high temperature protective coating alone [8-10]. MCrAlY coating has been widely used both as high temperature protective coating and as BC of TBCs due to its anti-oxidation and hot corrosion properties.

[*] Corresponding author: zhangyanfei@qlu.edu.cn

Thermal spraying technology is widely used in aviation, aerospace, petroleum, chemical industry, automobile, construction and many other fields due to its advantages of high efficiency, flexibility and low cost [11-12]. Plasma spraying is especially suitable for spraying ceramics and other high melting point materials because of its high flame temperature. The composition and thickness of the coating are easy to control, and the size and shape of the workpiece are less limited. It has become an important technical method for the preparation of TBCs in the field of surface engineering [13].

NiCrAlY material is the most commonly used thermal spraying superalloy material, which is widely used in surface protection and BC of TBCs [14-17]. Adding aluminum into NiCr alloy can form composite oxide film of Cr_2O_3 and Al_2O_3 at high temperature, which has low porosity, good toughness, firm adhesion, high melting point, good high temperature chemical stability, and excellent high temperature oxidation resistance and thermal shock resistance [18].

NiCoCrAlYTa alloy coating is generally used in harsh working environment, such as high temperature protection of aeroengine blade materials [19]. NiCoCrAlYTa alloy has more elements, Ni, Co and Cr are the main elements of the coating, Al and Y are the trace elements, and a small amount of Ta is added [20]. The effect of Ni and Co is to improve the corrosion resistance of the coating [21]. The presence of Co improves coating ductility and hot corrosion resistance. Al and Cr elements mainly determine the oxidation performance of the coating. Al element can combine with oxygen to form a dense protective film of Al_2O_3. Cr element can mainly improve the hot corrosion resistance of the coating, reduce the critical content of Al needed to form the Al_2O_3 film [22], and form the Cr_2O_3 film with slightly worse oxidation performance than that of Al_2O_3. Maintenance of the ratio of chromium and aluminum is critical to avoid coating embrittlement. A small amount of Y can increase the adhesion of surface oxide film. Ta can play the role of “oxygen absorption”, promote the formation of favorable oxides Al_2O_3 and Cr_2O_3, and improve the oxidation resistance and adhesion of the coating [23].

2. Methods and procedure

2.1. Preparation of coating

The feedstock powders of NiCrAlY powder (Amdry 962) and NiCoCrAlTaY (Amdry 997) were obtained from Oerlikon Metco (Winterthur, Switzerland). The composite coatings were fabricated by APS. Before APS, the substrates (45 steel) were sand blasted with corundum grits and then cleaned by ultrasonic cleaner with acetone. The process parameters of plasma spraying are shown in Table 1.

Table 1. Plasma spraying process parameters.

Powder	Amdry 962	Amdry 997
Current (A)	500	500
Voltage (V)	75	45
Primary gas pressure (Ar, PSI)	100	75
Primary gas flow (Ar, SCFH)	80	115
Power feed rate (% r.p.m)	35	25
Spray distance (mm)	130	150

The X-ray diffraction (XRD) patterns of the samples were obtained on D8-ADVANCE (AXS, Germany). Thermogravimetric differential thermal analysis (TG-DTA) of powder was performed on a STA 449F3 synchronous thermal analyzer (NETZSCH, Germany). The powders and coatings were impregnated with epoxy. After hardening of the resin, the sample was ground with SiC abrasive paper and polished on soft disks with diamond suspension. A cross section of the sample was investigated by SEM and Digital Microscope VHX-5000 (KEYENCE, Japan). GeminiSEM500/VP (CARL ZEISS, Germany) ultrahigh resolution emission scanning electron microscope was used to observe the changes of surface microstructure and powder particle size in the powder and coating before and after spraying.

3. Results and discussion

3.1. Surface morphology and composition of powders

3.1.1. Amdry 962

Figure 1 shows the surface morphology of gas atomized NiCrAlY powder (Amdry 962). The nominal composition is Ni22Cr10Al1.0Y. It can be seen from Figure 1a-c that the powder is spherical. It has good fluidity and smooth distribution, and is suitable for plasma spraying process. Some powders have dendritic structures on the surface (Figure 1c-d). The energy dispersive spectrometry (EDS) element mapping of the NiCrAlY powders is shown in Figure 1e. Composition of the powders are homogeneous and the phases are uniformly distributed.

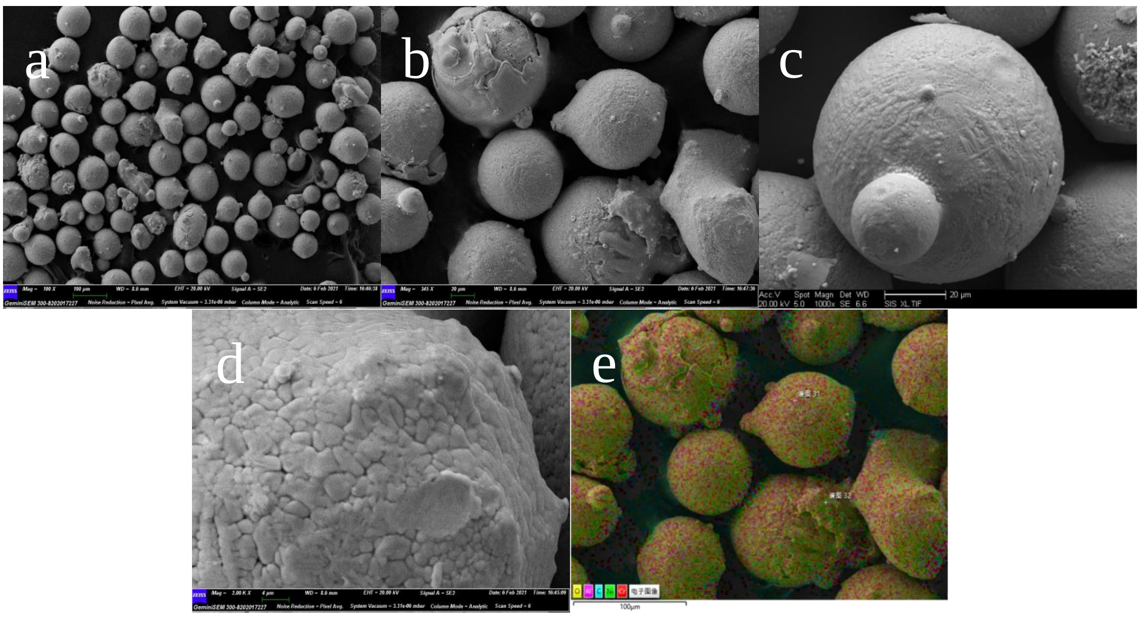

Fig. 1. SEM micrographs of Amdry 962 powder.

The powder morphology is consistent with the characteristics of gas atomization. The basic principle of gas atomization is to use a high-speed air flow to crush the liquid metal flow into small droplets and solidify them into powder [24].

NiCrAlY coating prepared with this powder has compact structure, high bonding strength, corrosion and cavitation resistance, and excellent oxidation resistance. NiCrAlY coating can be used as high temperature resistant coating, and can also be used as BC of TBCs.

3.1.2. Amdry 997

Figure 2 shows the surface morphology of gas atomized NiCoCrAlTaY powder (Amdry 997). The nominal composition is Ni23Co20Cr8.5Al4Ta0.6Y. It can be seen that the atomized alloy powder is spherical particle with regular and smooth shape. The as-cast dendrite structure also exists on the surface of the powder (Figure 2c-e). Figure 2f shows the EDS element mapping of NiCoCrAlTaY powder. It can be seen that the phase distribution is uniform.

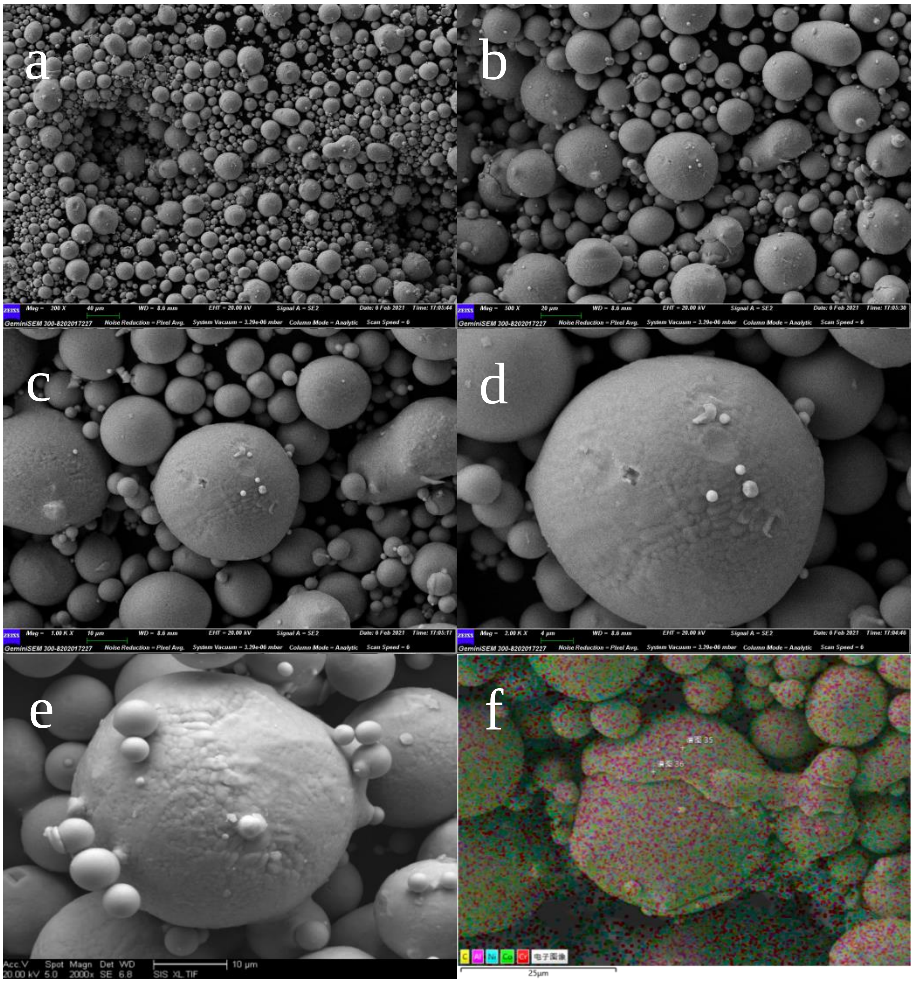

Fig. 2. SEM micrographs of Amdry 997 powder.

3.2. Cross section and EDS analysis of powders

3.2.1. Amdry 962

Figure 3 shows the image of Amdry 962 powder cross section. It can be seen that composition of the powders are homogeneous. This shows that the gas atomization method can make the powder get good uniformity.

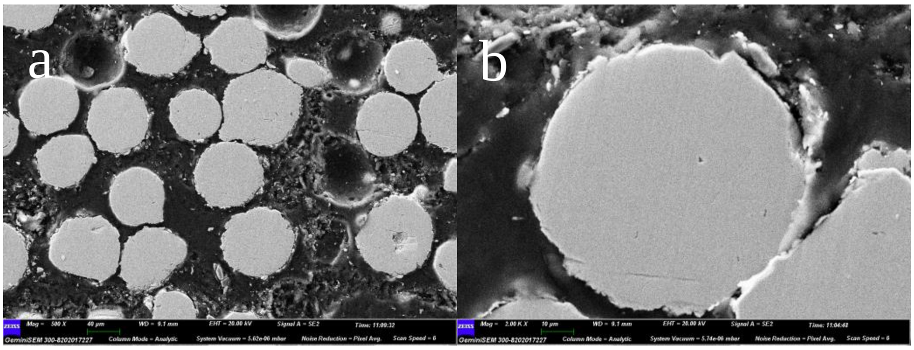

Fig. 3 Cross-section of Amdry 962 powder.

3.2.2. Amdry 997

Figure 4 shows the image of Amdry 997 powder cross section. It can be seen that the powder cross section of Amdry 997 is similar to that of Amdry 962. The two kinds of powder are prepared by gas atomization, so the composition of Amdry 997 is also very homogeneous.

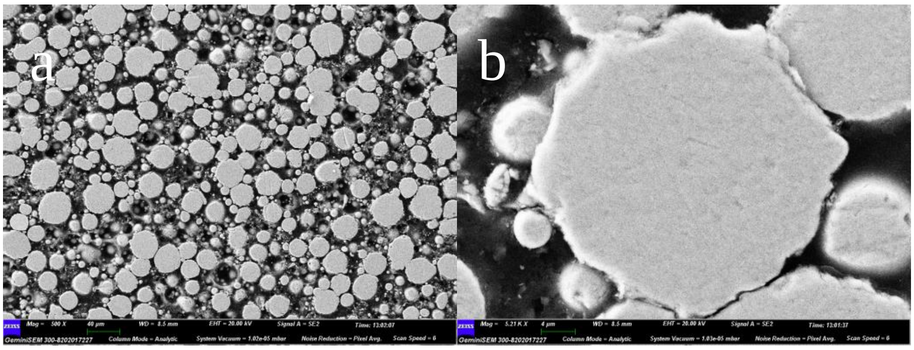

Fig. 4. Cross-section of Amdry 997 powder.

3.3. Surface morphology and composition of coatings

3.3.1. Amdry 962

Figure 5 shows the morphology of the Amdry 962 coating surface and its different areas. It can be seen from Figure 5a that the powder melting effect is good. NiCrAlY powder particles are well spread on the matrix, and the bonding between the powders is compact. There are few pores. The coating is a typical layer structure.

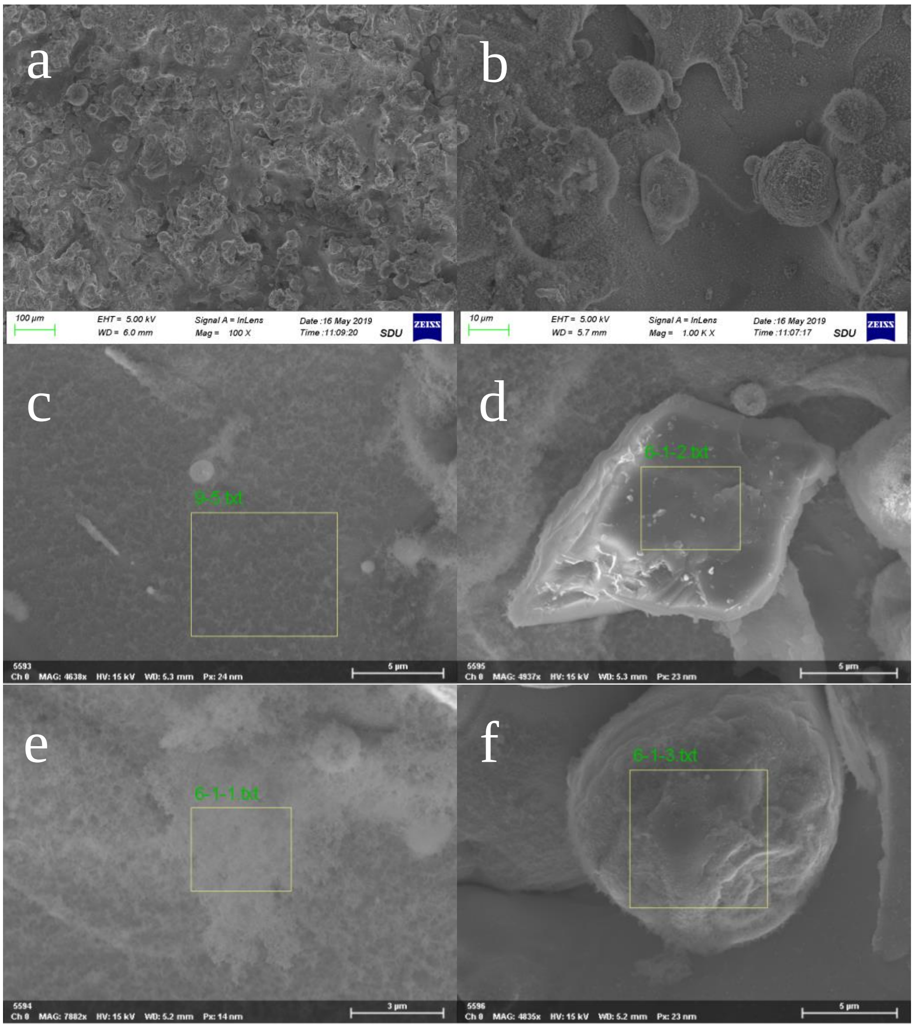

Fig. 5. SEM images of Amdry 962 coating surface morphology and its different areas: (c) smooth surface area, (d) block area, (e) flocculation area, (f) globular region.

Table 2. Chemical composition of smooth area in Figure 5c.

Element	Al	Cr	Y	O	Ni	Matrix
Wt%	40.66	33.80	14.98	2.45	8.11	100
At%	57.60	24.85	6.44	5.83	5.28	100

Table 3. Chemical composition of block areas in Figure 5d.

Element	Al	Cr	Y	O	Ni	Matrix
Wt%	61.69	0.78	0.71	35.85	0.96	100
At%	50.07	0.33	0.18	49.07	0.36	100

Table 4. Chemical composition of flocculent region in Figure 5e.

Element	Al	Cr	Y	O	Ni	Matrix
Wt%	45.34	29.48	7.30	10.87	7.01	100
At%	53.72	18.12	2.62	21.71	3.82	100

Table 5. Chemical composition of globular region in Figure 5f.

Element	Al	Cr	Y	O	Ni	Matrix
Wt%	58.45	19.17	5.64	12.18	4.56	100
At%	63.03	10.72	1.85	22.12	2.26	100

Figure 5b shows the existence of unmelted particles. There is a small amount of spherical structure in the coating, which is formed by the splashing of melted powder upon impact. It can be seen from Figure 5c that the melting effect of smooth surface area is good. The main compositions are Al and Cr, and there is a small amount of O element. EDS shows that the main composition of the block area (Figure 5d) is Al_2O_3. And the oxidation phenomenon is serious. Al_2O_3 and Cr_2O_3 are the main conpositions in flocculent area (Figure 5e) and globular area (Figure 5f).

3.3.2. Amdry 997

Figure 6 shows the morphology of the Amdry 997 coating surface and its different areas. It can be seen from Figure 6a that it is a typical plasma spraying coating, and the surface is composed of melted and unmelted particles. The particles are well spread and flattened, so the porosity of the coating is low. There are a lot of small particles on the surface of the coating, which may be caused by the splashing of molten particles during the spraying process. Figure 6b shows a large number of unmelted particles on the surface of the coating. EDS shows that the content of Ni is relatively high in the smooth surface area (Figure 6c). The globular area (Figure 6d) is seriously oxidized, and there are many kinds of oxides. There are no Cr and Ta elements in some long strip regions (Figure 6e), but only Ni, Co, Al, Y and O elements. EDS element mapping (Figure 6f) indicates that composition of the coating surface is homogeneous.

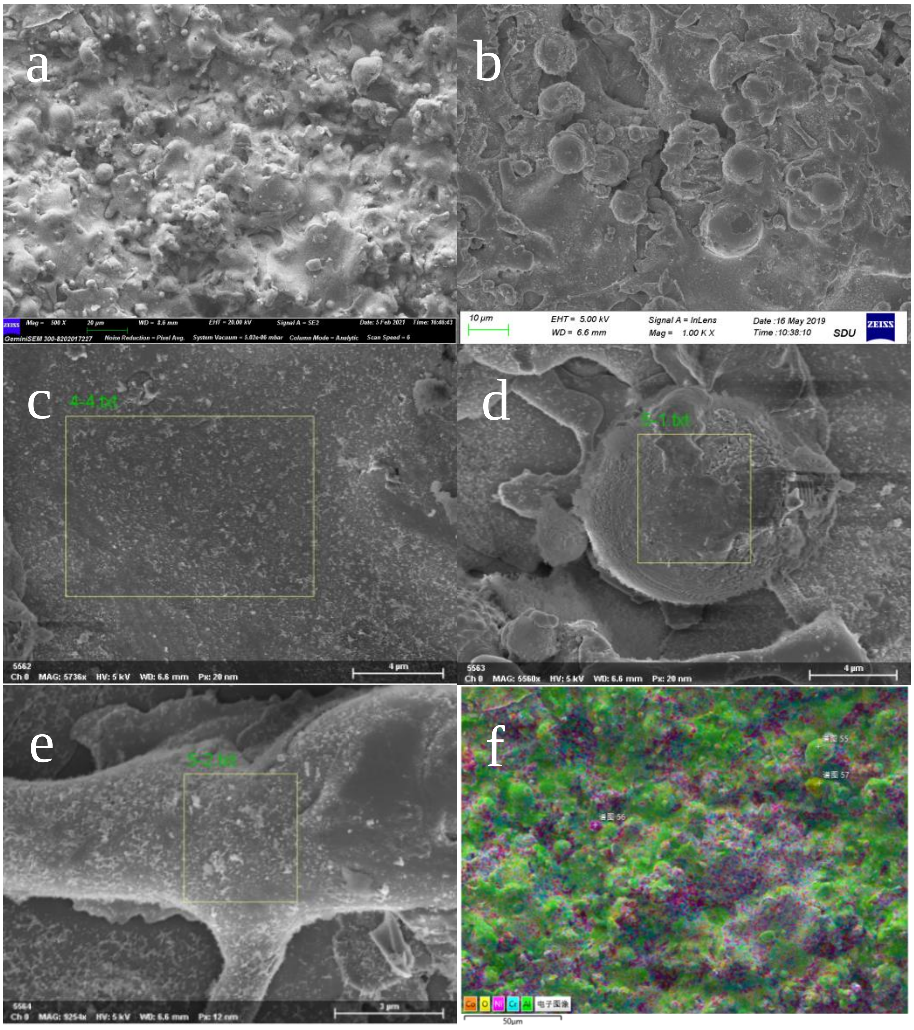

Fig. 6. SEM images of Amdry 997 coating surface morphology and its different areas: (c) smooth surface area, (d) globular region, (e) strip area.

Table 6. Chemical composition of smooth area in Figure 6c.

Element	Ni	Al	Cr	Co	C	O	Y	Ta	Matrix
Wt%	54.42	10.15	13.80	12.60	2.13	1.87	3.35	1.68	100
At%	43.65	17.72	12.50	10.07	8.37	5.49	1.77	0.44	100

Table 7. Chemical composition of globular region in Figure 6d.

Element	O	Al	Cr	Ni	Co	Y	Ta	Matrix
Wt%	28.32	17.96	26.84	14.91	7.06	3.18	1.72	100
At%	52.51	19.74	15.31	7.53	3.55	1.06	0.28	100

Table 8. Chemical composition of strip area in Figure 6e.

Element	Ni	Al	O	Co	Y	Matrix
Wt%	58.32	25.60	7.95	5.34	2.79	100
At%	38.79	37.05	19.40	3.54	1.23	100

3.4. Cross section and EDS analysis of coatings

3.4.1. Amdry 962

Figure 7 shows the image of Amdry 962 coating cross section. It can be seen that the melting effect of the coating material is good, it is a typical layered staggered structure. This is due to the spreading effect when the melted powder impacts on the substrate. The existence of unmelted particles in the coating (Figure 7b) may be due to low spraying power or short heating time of powder. In addition, the pores (Figure 7b-c) in the coating are caused by the overlapping of these unmelted particles. Figure 7d is the EDS element mapping of the coating cross section. It can be seen that the main composition of the coating is Ni. The existence of O in the coating indicates that the coating is oxidized during APS.

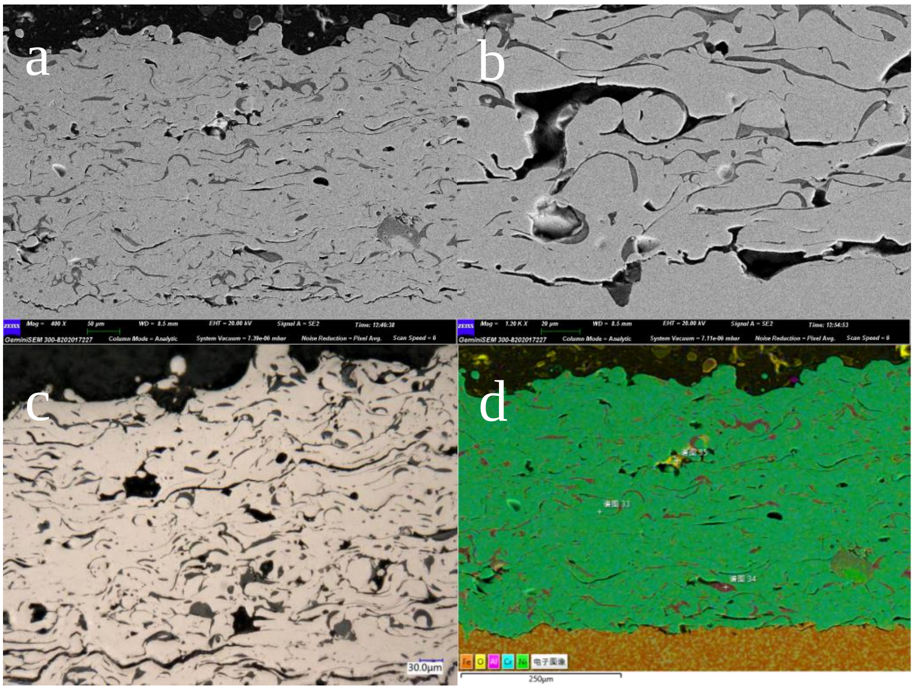

Fig. 7. Cross-section of Amdry 962 coating.

3.4.2. Amdry 997

Figure 8 shows the image of Amdry 997 coating cross section. It can be seen that the coating is a typical layered structure prepared by plasma spraying process. This is due to the spreading effect when the melted powder impacts on the substrate. The coating is closely combined with the substrate, without obvious cracks. It can be seen that there are unmelted particles in the coating (Figure 8b). The formation of unmelted particles is also caused by insufficient spraying power, short powder heating time or long particle flying time. Figure 8d shows the EDS element mapping of the Amdry 997 coating cross section. It can be seen that even if there are unmelted particles, the coating is uniform, because the powder composition is uniform.

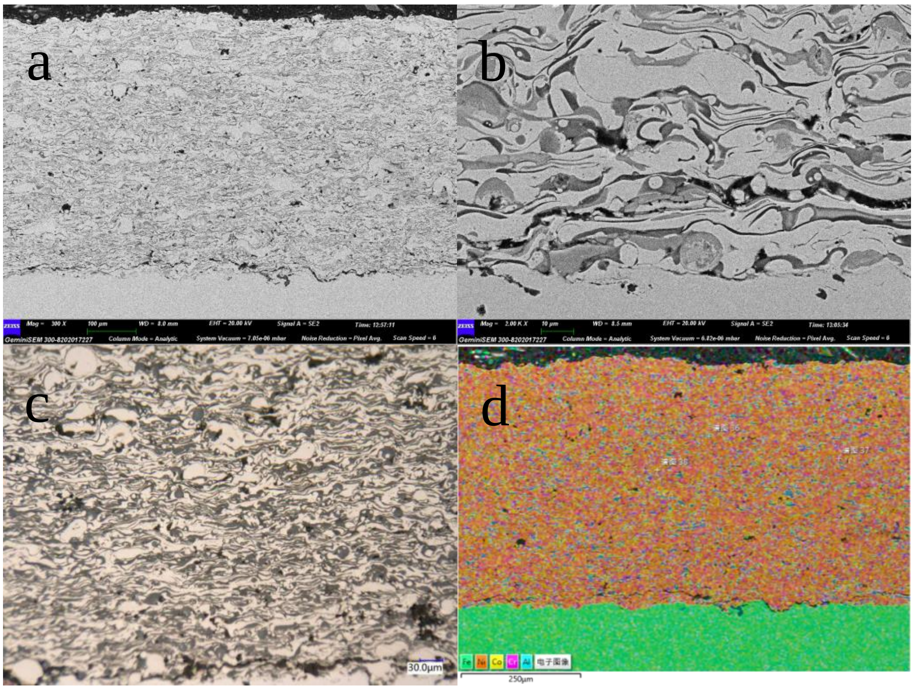

Fig. 8. Cross-section of Amdry 997 coating.

3.5. TGA Analysis

3.5.1. Amdry 962

Figure 9 shows the TG-DTA curves of the Amdry 962 powder. The melting points of Ni, Cr, Al and Y are 1455 °C,1857 °C, 660 °C and 1522 °C, respectively. The endothermic peak at 660 °C of the DTA curve corresponds to the melting of Al. Weight increase in TG curve from 200 °C to 1000 °C is due to the oxidation of elements such as Ni and Al. The powder is almost stable below 884 °C, above 884 °C powder weight increase dramatically indicating serious oxidation.

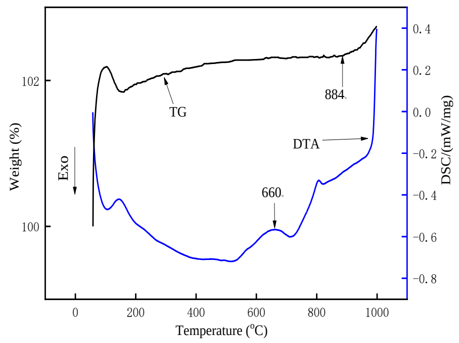

Fig. 9. TGA - DTA curve of the Amdry 962 powders.

3.5.2. Amdry 997

Figure 10 shows the TG-DTA curves of the Amdry 997 powder. The melting points of Ni, Co, Cr, Al, Y and Ta are 1455 °C, 1495 °C, 1857 °C, 660 °C, 1522 °C and 2996 °C, respectively. Weight increase in TG curve from 200 °C to 1000 °C is also due to the oxidation of elements such as Ni and Al. The powder is almost stable below 808 °C, above 808 °C powder weight increase dramatically indicating serious oxidation. So the maximum service temperature of Amdry 997 (808 °C) should be a little bit lower than that of Amdry 962 (884 °C).

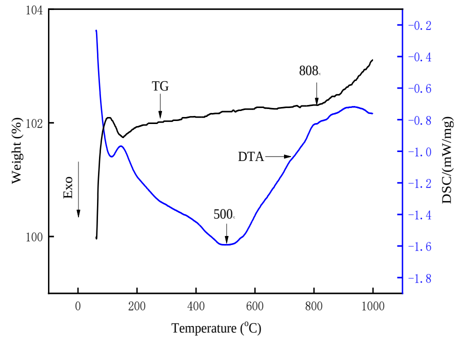

Fig. 10. TGA - DTA curve of the Amdry 997 powders.

3.6. XRD Analysis

3.6.1. Amdry 962

Figure 11 shows the XRD pattern of Amdry 962 powder and coating prepared by APS. Compared with the standard card, three peaks with the highest intensity correspond to the three main peaks of γ'-$AlNi_3$ (Tetragonal, PDF#50-1265). However, the diffraction peaks of Amdry 962 powder shift toward lower angles. In particular, the peak at about $2\theta = 74°$ shift toward lower angles seriously.

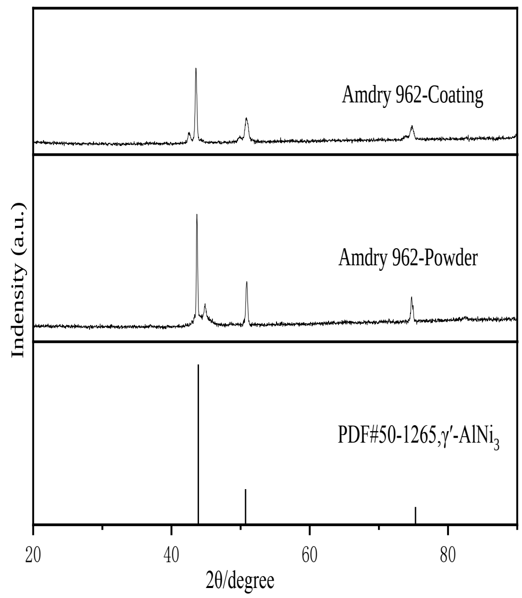

Fig. 11. The XRD spectra of Amdry 962 powder and coating.

3.6.2. Amdry 997

Figure 12 shows the XRD pattern of Amdry 997 powder and coating prepared by APS, as well as the standard card of $Al_{0.34}Co_{0.41}Cr_{0.2}$ (PDF#50-1290) and $Al_{0.1}Ni_{0.9}$ (PDF#44-1187) for references. The main phase of the powder is NiAl composite phase. The XRD pattern of Amdry 997 powder can match with β-$Al_{1.1}Ni_{0.9}$ (Cubic, PDF#44-1187). Compared with the standard card, the diffraction peaks of coating shift toward higher angles. The diffraction peaks of coating can match with $Al_{0.34}Co_{0.41}Cr_{0.2}$ (PDF#50-1290). It also match with Ni (Cubic, PDF#65-0380) and Cr (Cubic, PDF#06-0694). It can also match with many NiAl composite standard cards, such as $AlNi_3$ (Cubic, PDF#65-0430) and $Al_{0.42}Ni_{0.58}$ (Cubic, PDF#44-1267).

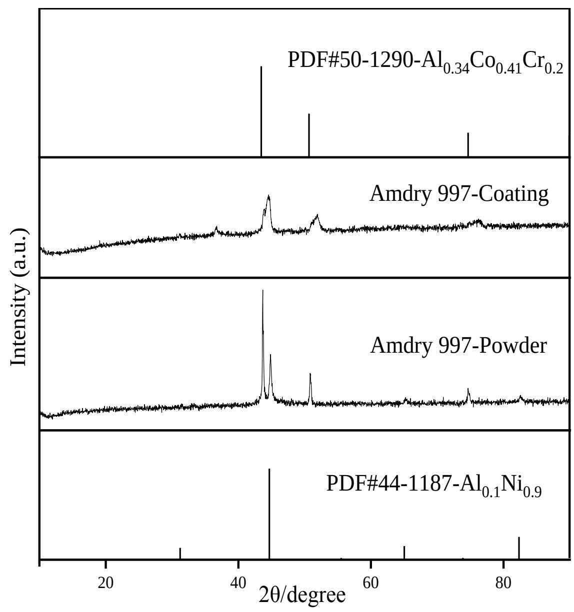

Fig. 12. The XRD spectra of Amdry 997 coating and powder.

4. Conclusions

The MCrAlY coating was prepared by atmospheric plasma spraying. The MCrAlY coating prepared from NiCrAlY powder and NiCoCrAlY powder were studied by SEM and XRD. The analysis shows that the melting effect of the two kinds of powder by plasma spraying is good, and the composition of the coating is homogeneous. Because the original powder composition is homogeneous, the coating composition is still homogeneous even though there are unmelted particles in the coating. Both coatings are oxidized during spraying, so there is a dense protective film on the surface of the coating to improve the oxidation performance of the coating. TG-DTA indicates that the maximum service temperature of Amdry 997 (808 °C) should be a little bit lower than that of Amdry 962 (884 °C). The main composition of NiCrAlY coating is γ'-Ni_3Al, while NiCoCrAlYTa coating contains several kinds of NiAl composites. Other properties such as hardness and abrasion resistance will be studied further.

Acknowledgements

This work was supported by “20 Policies about Colleges in Jinan” program (Grant NO: 2019GXRC047) and "migratory bird like" high level talent program in Tianqiao District.

References

[1] J. M. Liu, M. Y. Ch et al., Thermal Spray Technology **2**(04), 30 (2010).
[2] H. R. W, Heat Treatment of Metals Abroad **5**, 17 (2003).
[3] D. G. Lees et al., Oxidation of Metals **38**(3-4), 217 (1992).
[4] Kolarik Czech, Quadakkers et al., Surface Engineering **13**(5), 384 (1997).
[5] W. Lih, W. Chang et al., Oxidation of Metals **38**(112), 99 (1992).
[6] W. Brandl et al., Surface & Coatings Technology **86**, (1996).
[7] X. M. Peng, Ch. Q. Xia et al., The Chinese Journal of Nonferrous Metals **23**(11), 3147 (2013).
[8] X. M. Peng, Ch. Q. Xia et al., The Chinese Journal of Nonferrous Metals **18**(4), 601 (2008).
[9] Zh. L. Tang, F. H. Wang, W. T. Wu, Surface and Coatings Technology **99**(3), 248 (1998).
[10] X. M. Peng, Ch. Q. Xia. K. Ma et al., Materials Chemistry and Physics **107**(1), 158 (2008).
[11] B. Sh. Xu, Sh. C. Liu, Surface Engineering, 2000.
[12] X. D. Chen, W. Zh. Han, Surface Coating Technology **40**, (1997).
[13] Ch. X. Li, H. X. Yin et al., Materials Protection **42**(04), 59 (2009).
[14] H. R. Wang, Heat Treatment of Metals Abroad **24**(5), 17 (2003).
[15] D. Q. Yu, X. Y. Lu, J. Ma, Acta Metallurgica Sinica **48**(6), 759 (2012).
[16] Ch. X. Li, T. T. Xu, N. Xu, Materials Protection **43**(3), 11 (2010).
[17] W. Zh. Li, Y. Q. Li, D. Q. Yi et al., The Chinese Journal of Nonferrous Metals **23**(2), 417 (2013).
[18] Y. F. Zhang, Technology Innovation and Application **11**, 128 (2015).
[19] K. S. Zh, X. H. Liang, M. Liu, The Chinese Journal of Nonferrous Metals **19**(3), 15 (2009).
[20] X. B. Wu, South China University of Technology, 2014.

[21] Ch. Sh. Hu, F. H. Wang, Corrosion Science and Protection Technology **1**2(3), 160 (2000).
[22] A. M. Huntz, Materials Science & Engineering **87**, 251 (1987).
[23] L. Q. Wang, X. Y. Song, New Technology & New Process **3**, 34 (2002).
[24] Sh. Q. Chen, B. Y. Huang, Powder Metallurgy Technology **5**, 297 (2004).